



## A Strong Ground Motion Catalogue of Selected Records for Shallow Crustal, Near Field Earthquakes in Iran

Maryam Sedghi<sup>1,2</sup>, Arezou Dorostian<sup>\*1</sup>, Mehdi Zare<sup>3</sup>, Mohsen Pourkermani<sup>1</sup>

1. Department of Geology, North Tehran Branch, Islamic Azad University, Tehran, Iran

2. Iranian Red Crescent Society (IRCS), Tehran, Iran

3. International Institute of Earthquake Engineering and Seismology (IIEES), Tehran, Iran

Received 10 March 2019; accepted 15 October 2019

### Abstract

Understanding strong ground motions in the near-fault areas is important for seismic risk assessment in densely populated areas. In the past, lack of information on strong ground motion for large and moderate earthquakes led to the use of mainly far field large and moderate earthquake records in equations for calculation of the strong ground motion parameters. In this article, we collected and generated a seismic catalogue with a data set of corrected and processed 217 triaxial near source strong ground motion and accelerometric data recorded from 1976 to 2018 obtained from 30 shallow crustal earthquakes with a focal depth below 30 km from different regions including 24 in Iran, 5 in California and one in Italy (because of the lack of Iranian near-field accelerograms) in different stations. These data were recorded (129 Iranian records, 88 from California and Italy) with a source-to-site distance less than 80 km and earthquakes between  $M_w = 5$  and 7.5. Receiver function method was used for site classification for these records. The percentage of processed data in this study was 18%, 43%, 33% and 6% for the different site classes of 1, 2, 3, and 4. In the final catalog, records in which their  $PGA \geq 100 \text{ cm/s}^2$ , were reported. This near source ground motion database also contains information about ground motion, source parameters and is fundamental for dynamic research in earthquake engineering for the estimation of strong ground motion parameters (PGA, PGV, PGD and frequency content of response spectra) of moderate-to-large earthquakes.

**Keywords:** Catalogue, Near Fault, Strong motion, Earthquake

### 1. Introduction

One of the most significant tools in seismology is seismicity catalogues. They provide comprehensive data used for research on seismicity, seismotectonics, physics of earthquake, seismic hazard analysis, ground-motion prediction equations, determination of long-term seismic strain rates. For example ASMI, (Archivio Storico Macrosismico Italiano), will represent the Italian node of the European Archive of Historical Earthquake Data (AHEAD). ASMI released more than 5000 Italian earthquakes, 20000 records on about 6000 earthquake. Texts, tables about descriptions of the earthquake effects, earthquake parameters and also the practical maps, showing the location of earthquakes epicenter, included in this archive and allows users to compare and interpret existing studies. The United States Geological Survey (USGS) catalogs also represents a synthesis of catalog information from many sources into simple one-line catalog entries of date, time, location, and selected estimate(s) of earthquakes size that occurs worldwide and United States. Some other catalogs represent average annual statistics for earthquake counts. U.S. and worldwide deaths per year. According to (Chu and Gordon 1998), there is a complex interaction between the African, Saudi Arabian and Eurasian tectonic plates. The opening of the Red Sea rift between the Arabian and North African plates is due to the expansion of the

Red Sea and the spreading rate of approximately 10mm/yr. The active tectonics of the Himalayan-Alpine belt has formed the Iranian plateau, which lies at the convergence boundary between the Eurasian Arabian plates. This plateau is one of the most seismically active area in the world and faces earthquakes every year. Moderate to strong earthquakes, with magnitudes of up to 7, have been historically recorded for many active faults in Iran.

Many populated urban centers and industrial complexes have been developed near mountain foothills that are usually bordering active faults, so high magnitude earthquakes along such faults have destroyed many cities and caused large economic and human loss (Ambraseys and Melville 1982). Near-fault ground motions are characterized by a short-duration impulsive motion that exposes the structure to high input energy at the beginning of the record. The gradually increasing number of recorded near source time histories has recently enabled strong motion seismologists to analyze more precisely the character of the near-fault ground motions and therefore contribute to the physical understanding of those features that control them (Campillo et al., 1989; Somerville and Graves, 1993; Abrahamson and Somerville, 1996; Oglesby and Archuleta, 1997; O'Connell et al., 2007). Literature review shows the reports on the gradual improvement of theoretical relationships between strong motion and earthquake source parameters (Aki 1968; Haskell 1969;

\*Corresponding author.

E-mail address (es): [dorostian382@yahoo.com](mailto:dorostian382@yahoo.com)

Boore and Zoback 1974; Levy and Mal 1976; Israel and Kovach 1977; Hartzell 1978; Bouchon 1979). Another way to determine earthquakes focal depth is detailed analysis of teleseismic waveforms. Earthquakes with  $M \geq 5.2$  have relocated in the International Seismological Center (ISC) catalogue by Engdahl et al. (1998). Focal depth of events has been relocated by (Maggi et al. 2002)

The moment magnitude of earthquakes collected from Iran, California and Italy (to complete the catalog due to the lack of near fault data in Iran and also the tectonic similarity between the California, Italy earthquakes with earthquakes in Iran), are greater than 5.5 and below 7.5 and a close source to site distances less than 80 km. Figure 1 shows the map of epicenters of 24 large earthquakes occurred in Iran, for which the 129 Iranian records are selected and studied in this paper.

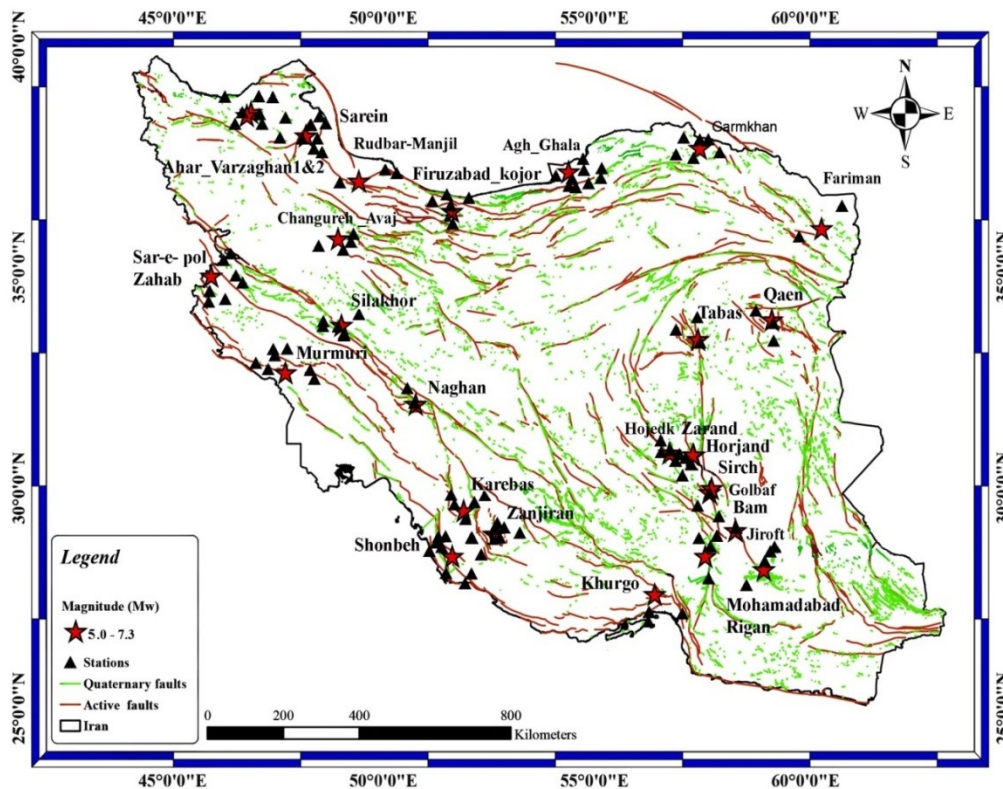


Fig 1. Epicenters of 24 large earthquakes occurred in Iran and 129 records that are analyzed in this paper (listed in Table 1).

The recent powerful shallow crustal earthquake with magnitude of 7.3 happened in November 12, 2017 in the west of Iran in Kermanshah Province, Sarpol-e-zahab region, which had a large aftershock zone, and Kerman Province sequential earthquakes during the last year, are cases mentioned in this study. The analysis of these records for discovering physical properties of the earth is important in these regions for the purposes of engineering and structural design, compilation, and updating building codes.

The application of near-source distances ( $R \leq 80$  km) is of great importance due to the influence of such distances in seismic hazard analysis (Campbell and Bozorgnia 2013). They also used rupture distances less than 80 km to develop their Ground Motion Prediction Equations (GMPEs) and set distances less than 80 km as near-source distances. Another point to be noted here is

the similarity of the shallow earthquakes occurred in the region of Iran and California. Shallow crustal earthquakes on destructive plate boundaries had casualties and also occurred in places that had experienced earthquakes before. The California-Nevada region has about 90 percent of the seismic activity of the United States (Fig 2), a result based mainly on present conditions, but in good agreement with historical data (Gutenberg and Richter 1944). It should be noted that Italy is also one of the most seismically active Mediterranean regions, where a long history of earthquakes has strongly influenced the development of earthquake-resistant structural design. These earthquakes are almost confined to the first 20 km of depth. Italy has frequently experienced strong shaking induced by earthquakes with a magnitude of 5.0 or greater.



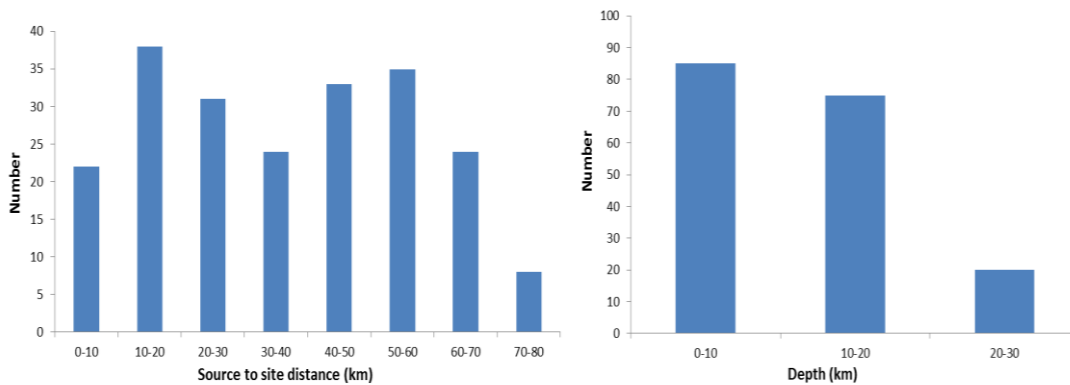


Fig 3. Distribution of depth and source to site distance versus the number of records.

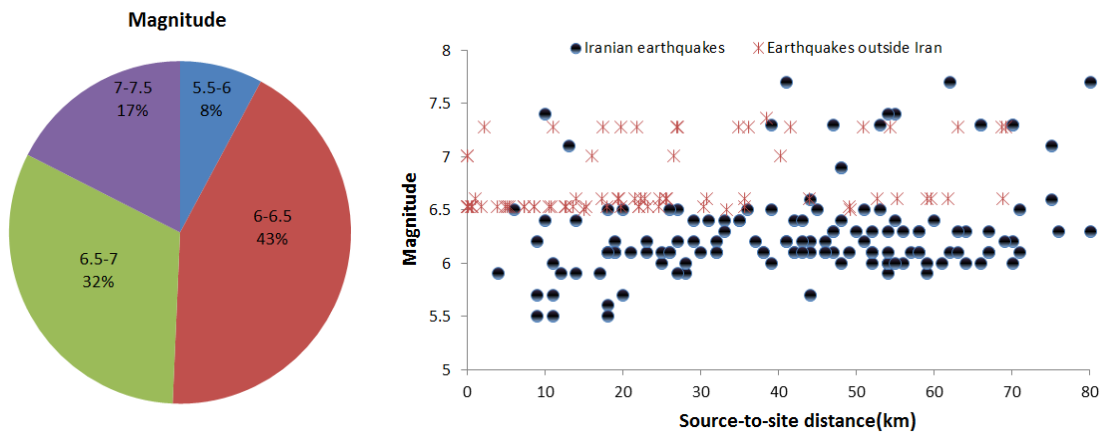


Fig 4. Distribution of strong ground motion data used in this research, according to moment magnitude, source to site distance and number

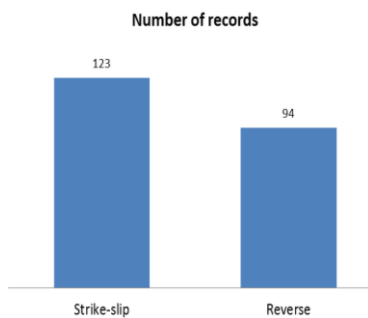


Fig 5. The distribution of style of faulting against the number of records

Focal mechanisms began to be computed from the first motions on a routine basis following the establishment of the World-Wide Standardized Seismograph Network (WWSSN) seismic network in the early 1960s. These results confirmed the double-couple theory for earthquake sources and showed that the earthquake mechanisms in different regions were consistent with

the emerging theory of plate tectonics. Most of earthquakes are studied in this paper have strike-slip and reverse mechanisms or a combination of these two modes (Harvard, seismology web site, 2003, National Earthquake Information Center (NEIC) web site, 2003).The source specifications for these earthquakes and strong-motion records are listed in Tables 1 and 2.

**2.2. Correction procedure for records**

Generally, the aims for processing the raw data obtained from recording instrument are as follows: a) correction according to the instrument characteristic curve; b) correction of the high and low frequency errors to reduce random noise in the recorded signals; c) filtering of frequency content to maintain or highlight a part of data. Data correcting procedure of strong ground motion records leads to the creation of useful data in engineering analysis. In the frequency domain, the Fast Fourier Transform (FFT), as one of the pillars of filtering algorithms, is used for these operations.

Table1. The selected Iranian earthquakes, Focal mechanisms; as reported by Harvard CMT catalog (HRV) and Focal depth by (USGS) and Maggi et al. (2002)

No	Name of earthquake	Date (dd/mm/yyyy)	Time (UTC)	Epicentral lat°N (degree)	Epicentral long°E (degree)	M <sub>w</sub>	Focal Depth (km)	Nodal Plane				Mechanism	Moment Tensor (N-m)
								Plane	Strike	Dip	Rake		
1	Agh_ghala	10/7/2004	21:46:20	37.125	54.477	6.2	32.0	NP1 254°	55°	122°	Reverse	3.220e+17	
								NP2 27°	46°	53°			
2	Ahar_varzaghan	11/08/2012	12:23:18	38.329	46.826	6.1	11.0	NP1 173°	74°	1°	Strike-slip	6.290e+18	
								NP2 82°	89°	164°			
3	Bam	26/12/2003	01:56:52	28.995	58.311	6.5	10.0	NP1 269°	87°	41°	Strike-slip	8.637e+18	
								NP2 176°	49°	175°			
4	Changoreh_avaj (Bou'in-Zahra)	22/06/2002	02:58:21	35.626	49.047	6.4	10.0	NP1 276°	32°	66°	Reverse	5.759e+18	
								NP2 123°	61°	104°			
5	Corebas	1999/05/06	23:00:53	29.501	51.880	6.1	33.0	NP1 143°	84°	-165°	Strike-slip	2.498e+18	
								NP2 52°	75°	-6°			
6	Firoozabad_kojur (Baladeh)	28/05/2004	12:38:44	36.290	51.610	6.3	17.0	NP1 319°	67°	98°	Reverse	3.653e+18	
								NP2 119°	24°	72°			
7	Garmkhan	04/02/1997	10:37:47	37.661	57.291	6.5	15	NP1 328°	81°	-171°	Strike-slip	6.723e+18	
								NP2 236°	81°	-9°			
8	Ghaen	11/07/1976	04:00:51	33.802	59.155	6.2	13	NP1 260°	78°	6°	Strike-slip	1.09e+25	
								NP2 169°	84°	168°			
9	Golbaf	11/6/1981	07:24:25	29.913	57.715	6.6	31	NP1 269°	85°	53°	Reverse	9.82e+25	
								NP2 172°	37°	171°			
10	Hojdek	12/12/2017	08:43:18	30.737	57.280	6.1	12	NP1 312°	51°	95°	Reverse	1.388e+18	
								NP2 124°	39°	84°			
11	Horjand	1/12/2017	02:32:46	30.746	57.307	6.1	13	NP1 320°	45°	109°	Reverse	1.505e+18	
								NP2 115°	48°	72°			
12	Khorgoo	21/03/1977	21:18:54	27.609	56.393	6.6	29	NP1 267°	27°	98°	Reverse	1.4e+26	
								NP2 78°	63°	86°			
13	Mohamadabad_rigan	27/01/2011	8:38:28	28.195	59.015	6.2	10	NP1 221°	85°	-167°	Strike-slip	2.423e+18	
								NP2 129°	77°	-5°			
14	Mormori	18/08/2014	02:32:05	32.703	47.695	6.2	10.02	NP1 310°	19°	100°	Reverse	2.915e+18	
								NP2 119°	72°	87°			
15	Roudbar_manjil	20/6/1990	21:00:09	36.957	49.409	7.4	18.5	NP1 19°	35°	179°	Strike-slip	1.776e+20	
								NP2 110°	90°	55°			
16	South_jiroft	04/03/1999	05:38:26	28.343	57.193	6.5	23	NP1 319°	13°	132°	Reverse	6.483e+18	
								NP2 97°	80°	81°			
17	Sarein	28/2/1997	12:57:18	38.075	48.050	6.1	10	NP1 184°	57°	-15°	Strike-slip	1.743e+18	
								NP2 283°	77°	-146°			
18	Sarpol_zahab	12/11/2017	18:18:17	34.911	45.959	7.3	19	NP1 351°	16°	137°	Reverse	1.124e+20	
								NP2 122°	79°	78°			
19	SE_fariman	05/04/2017	06:09:12	35.776	60.436	6.1	13.0	NP1 316°	20°	120°	Reverse	2.084e+18	
								NP2 105°	73°	80°			
20	Shonbeh	09/04/2013	11:52:49	28.428	51.593	6.3	12	NP1 313°	71°	85°	Reverse	5.536e+18	
								NP2 147°	20°	103°			
21	Silakhor	31/3/2006	01:17:00	33.500	48.780	6.1	7	NP1 313°	78°	-174°	Strike-slip	1.727e+18	
								NP2 222°	84°	-12°			
22	Sirch	28/07/1981	17:22:24	30.013	57.794	7	33	NP1 300°	79°	84°	Strike-slip	1.0 e+25	
								NP2 150°	13°	119°			
23	Tabas	16/09/1978	15:35:56	33.386	57.434	7.4	33	NP1 328°	33°	107°	Reverse	1.50 e+25	
								NP2 128°	59°	79°			
24	Zanjiran	20/6/1994	09:09:02	28.968	52.614	5.8	15	NP1 251°	67°	-5°	Strike-slip	8.05e+24	
								NP2 343°	85°	-157°			
25	Zarand	22/2/2005	02:25:22	30.754	56.816	6.5	14	NP1 266°	47°	100°	Reverse	5.375e+18	
								NP2 71°	44°	79°			

Table 2. The selected Californian and Italian earthquakes, from Pacific Earthquake Engineering Research Center (PEER), Focal mechanisms; as reported by Harvard CMT catalog (HRV) and Focal depth by (USGS).

No	Name of earthquake	Date (dd/mm/yyyy)	Time (UTC)	Epicentral lat°N (degree)	Epicentral long°E (degree)	M <sub>w</sub>	Focal Depth (km)	Nodal Plane				Mechanism	Moment Tensor (N-m)
								Plane	Strike	Dip	Rake		
1	Cape_Mendocino	25/04/1992	18:06:05	40.335	124.229	7.2	10.5	NP1 150°	47°	30°	Reverse	1.333e+19	
								NP2 38°	68°	133°			
2	Imperial_valley	15/10/1979	23:16:59	32.667	115.359	6.5	15	NP1 46°	90°	-51°	Strike-slip	2.50e+25	
								NP2 136°	39°	-180°			
3	Kern_County Landers	21/7/1952	11:52:14	34.958	118.998	7.5	6.0	NP1 51°	75°	61°	Reverse	9.2e+19	
		28/06/1992	11:57:34	34.200	116.437	7.3	1.09	NP1 69°	85°	-26°			
4	San_Fernando	09/02/1971	14:00:41	34.416	118.370°	6.6	9.0	NP2 161°	64°	-175°	Reverse	1.12e+24	
								NP1 67°	52°	72°			
5	Friuli_Italy	06/5/1976	20:00:12	46.356	13.275	6.5	9.0	NP1 284°	18°	119°	Reverse	5.70e+18	
								NP2 74°	74°	81°			
6	Cape_Mendocino	25/04/1992	18:06:05	40.335	124.229	7.2	10.5	NP1 150°	47°	30°	Reverse	1.333e+19	
								NP2 38°	68°	133°			

Actually, in physics, acceleration, velocity, and displacement can be converted to each other by integrating. Although this feature is not seen in many strong ground motion recordings, the double integration of a disseminated acceleration might not be the same as the corresponding disseminated displacement. Incompatibilities in data, not only cause changes in the waveform but also affect the response spectrum of the

acceleration parameter, and ultimately, fundamental problems arise in calculating the nonlinear response spectrum (Pecknold and Riddell 1978). Figure 7 shows an example of acceleration, velocity, and displacement plotted for the selected records. All raw records in this study were processed for three components of acceleration, velocity, and displacement, as illustrated in Fig. 8.

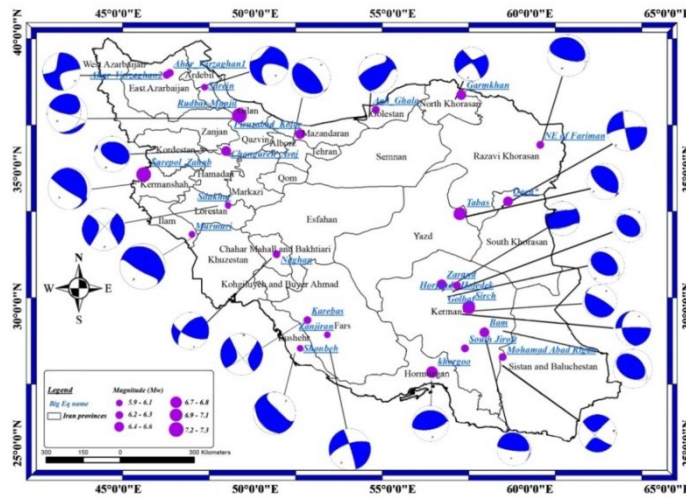


Fig 6. CMT (Harvard University) solutions obtained for territory of Iran.

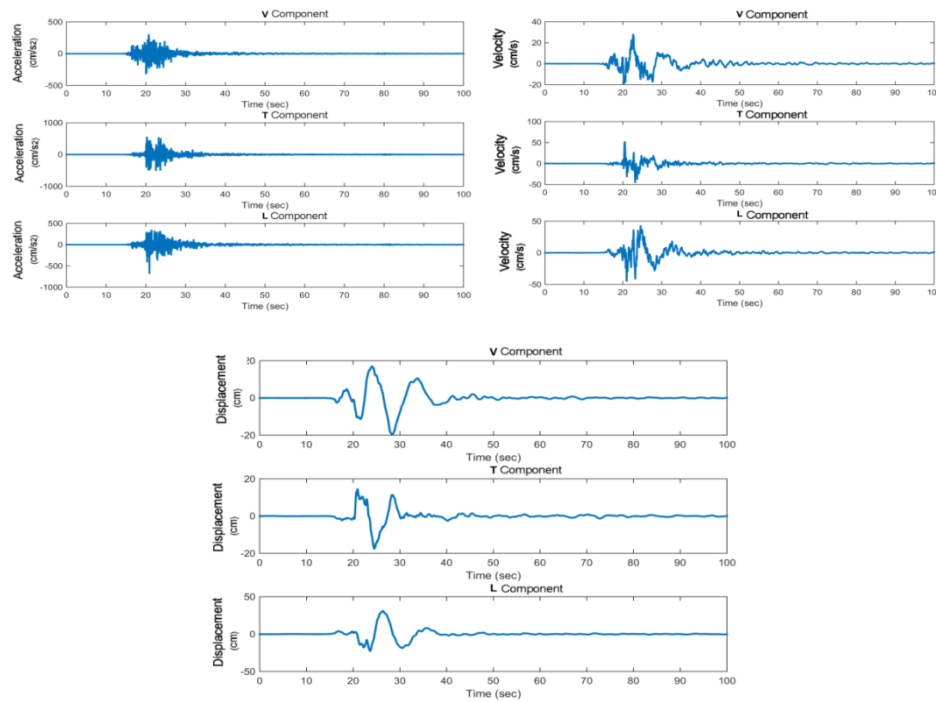


Fig 7. Acceleration, velocity, and displacement traces (Sarepolzhab station, 12/11/2017,  $M_w=7.3$ , Kermanshah earthquake).

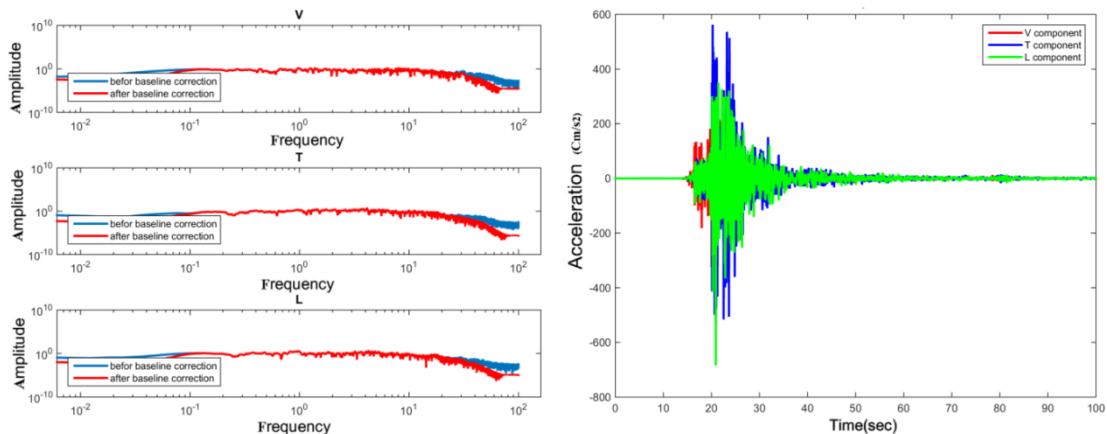


Fig 8. A sample of Time series of acceleration and The FFT in raw and corrected record, before and after baseline correction, for Sarepolzhab station, 12/11/2017,  $M_w=7.3$ , Kermanshah earthquake. V: vertical component, L&T are horizontal components.

The three-step algorithm includes least squares fitting in acceleration, high-pass filtering in acceleration, and subtracting of the initial value in the velocity. The first and third steps can effectively reduce the low-order (second or lower order) baseline errors, while the filtering reduces the residue of low-order noise and the high-order baseline errors that come from the background and instrument noises. The least squares fitting in the first step removes the linear trend in the acceleration. The second step requires a filtering in acceleration to remove the remaining errors and high-order random noise. If a proper high-pass filter is selected, the filtering can remove most of the errors in acceleration. Three possible approaches can be used to remove the effect of the initial velocity. For the processing of most digital strong-motion data, all three steps in the proposed algorithm are necessary.

Filter cutoff frequencies for each accelerogram are of tremendous importance which could simply alter values of PGA, PGV, and 5%-damped elastic pseudo-absolute acceleration response spectral ordinates PSAs (Akkar and Bommer 2007). For specifying these cutoff frequencies, the Fourier amplitude of the signal to the Fourier amplitude of the noise was plotted and applied in Fig 9.

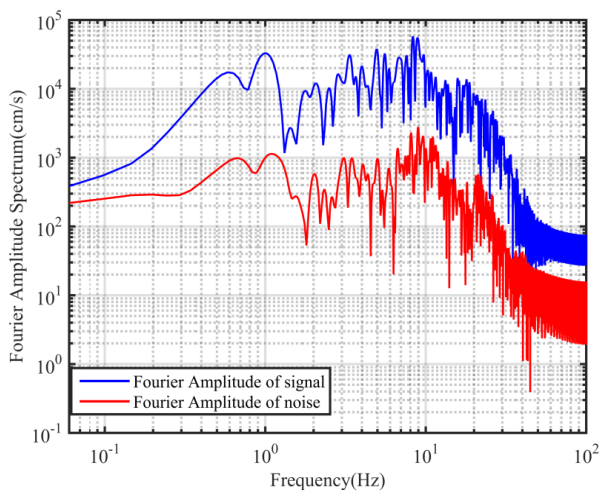


Fig 9. Comparison between FFT amplitude of the signal and the noise

### 2.2.1. Baseline correction

To remove the short and long period errors from accelerograms, the time-histories are often filtered. Originally the method for correction of such errors is done by subtracting a best-fit parabola from the accelerogram before the velocity and displacement values are calculated by integrating the acceleration values, but now high-pass filters and modern data processing techniques is used in this regard (Kramer 1996). Sophisticated baseline correction procedures are used in more complex cases of instrumental disturbances. Primary step is sub-dividing the velocity

signal into multiple ranges and use the least square regression. Figure 9 shows the FFT of the selected record before and after the baseline correction procedure. Each component of the strong ground motion records is analyzed by visual revision. The velocity data are obtained by integration of the accelerations and removing the long period component from the velocity function. The displacement data are obtained from the velocities in a similar manner.

### 2.2.2. Band pass filtering

The basis of the filters is the separation of the signals based on the frequency and the noise elimination. In many gathered data, the signal frequency is low and recorded data has low amplitude. Detection of this low-amplitude signal against high-amplitude noise in records is very difficult and usually the signal is buried. In this case, "low-pass filter" is used to reduce high frequencies. Therefore, the low frequencies can easily become visible. In fact, the "low-pass filter" is a filter that transmits low frequencies rather a set corner frequency and prevents the passage of high frequencies. A "high-pass filter" passes through frequencies higher than specified limit. When these two filters are set, the final filter is named as the "band-pass filter." In this study, we processed all selected records by the band-pass second order Butterworth filter, having  $SNR > 3.0$  (as shown in Fig 10) that are given in Table (3).  $SNR$  is the Signal to Noise Ratio. In this way, for each record, high and low frequencies ( $F_H$  &  $F_L$ ) were selected as shown in Fig 11.

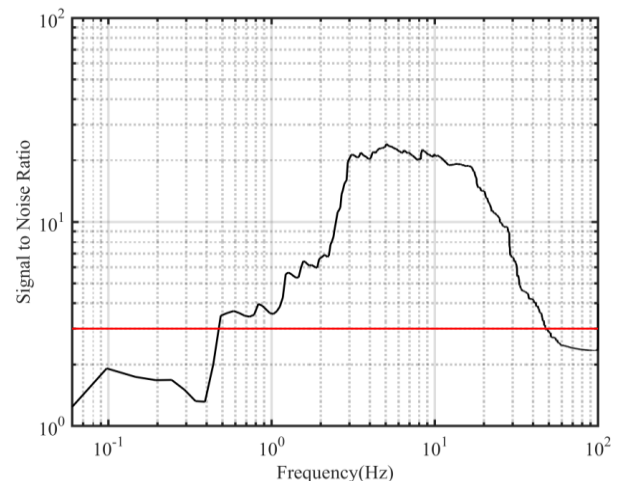


Fig 10. A sample of signal to noise ratio for , 12/11/2017, Mw=7.3, Kermanshah earthquake, Sarepolzhab station.

The records with  $SNR > 3.0$  for the frequency band less than ( $f_c$ ) and greater than  $f_{max}$  are taken and determined to be reliable for further study. ( $f_c$ ) represents corner frequency and  $f_{max}$  represents maximum frequency which is located at the end of the flat part of the acceleration spectra. It should be noted that  $SNR$  is estimated for each studied records (Fig 10).  $SNR$  is defined as follows (Theodulidis and Bard 1995):

$$SNR = (S(f)/\sqrt{t1})/(N(f)/\sqrt{t2}) \quad (2)$$

t1 and t2 represent the window length for the signal and noise sections. Because the records used in this study are digital records, (t2), was selected before the p-unset (mainly from 0 to 4 seconds, in the pre-event part of records) for noise parts.

**3. Site characterizations - H/V Method**

One key issue that required especial attention is that the local soil conditions influences the strong ground motions characteristics significantly. This is a very essential issue in the design of structures; that is why, many countries consider different design criteria for different soil types (Council 2000). Geotechnical hazards often occur as a result of earthquakes depending on site conditions and seismic characteristics. Deformation of the earth and irreparable damage to buildings are the result of this issue (Forootan et al. 2015). We classified local site conditions at each recording site into one of four categories defined as I, II, III, and IV, according to the Iranian code of practice (Code 2005) in estimating soil classes from  $V_{S30}$  (Table 3). The average shear wave velocity of upper 30 meters, despite the numerous weaknesses in expressing the dynamic properties of the site, is one of the most reliable parameters in earthquake classification in various regulations and seismic building codes in the world.  $V_{s, 30}$  is average shear (S) wave velocity in

different layers of soil to a depth of 30 meters from the base level, which is described below:

$$VS, 30 = \frac{30}{\sum_{i=1}^n \frac{h_i}{v_i}} \tag{3}$$

In this formula  $h_i$  and  $V_i$  are the thickness (m) and  $V_s$  is the shear wave velocity (m/s). Note that the method of H/V (Horizontal-to-Vertical spectral ratio) is one of the fast and useful methods for engineering purposes in determining the site characteristics. In this method, ambient noise wave measurement using three-component sensors is used on the ground surface. (Zaré 2007) pointed out in his paper that when the basic frequency was greater than 3 in the H/V spectral ratio, for the frequency bands of greater than 15Hz, site classes of 1, 5 to 15Hz, site classes of 2, 2 to 5Hz, site classes of 3, and less than 2Hz, site classes of 4 are assigned respectively. The H/V method was used to classify the soil in Iranian records, because of the lack of  $V_{S30}$  at some stations. In addition, at stations where  $V_{S30}$  was determined for them, a consistent and appropriate answer was also obtained for classification of soil type based from the H/V method. In this study, H/V ratio values for all records were calculated. For example, in Fig 12, the H/V ratio is plotted for Hojedk station,  $M_w=5.2$ , 02/12/2017, Horjand station with  $M_w=6.2$ , 01/12/2017 in Kerman Province and Sarpol-e-zahab station in Kermanshah Province recorded in 12/11/2017,  $M_w=7.3$ .

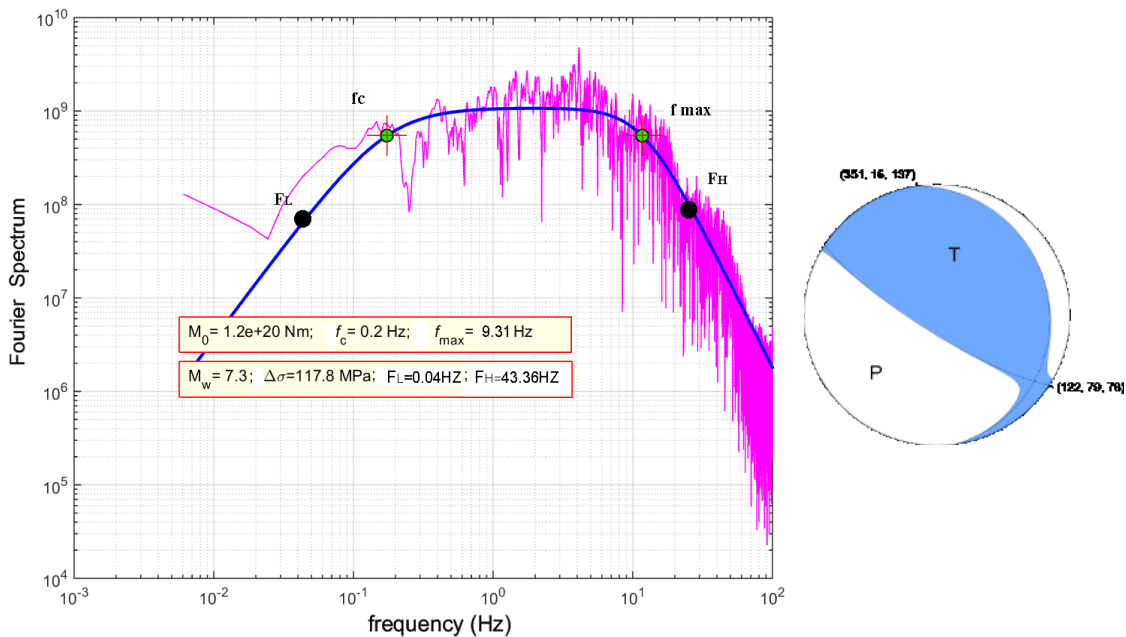


Fig 11. Determination of corner frequencies, low, and high frequencies band pass filtering from FFT of accelerations in selected record of, 12/11/2017,  $M_w=7.3$ , Kermanshah earthquake, Sarepolehahab station -Focal mechanism of earthquake.  $M_0$  is seismic moment,  $\Delta\sigma$  is stress drop.

#### 4. Discussion

Estimating the strong ground motion factors (peak acceleration, velocity, amplitude, and frequency content of response spectra) of moderate-to-large earthquakes is an important process for the seismic analysis of main engineering structures. In earthquake engineering and seismic analysis, estimating the strong ground motion parameters (peak ground acceleration, velocity, and displacement) is significant. These parameters are considered as key parameters in the design of vital structures. This catalog contains comprehensive information on the characteristics of digital accelerograms near fault recorded in different soil conditions in Iran. It can be used in applied studies in seismology and earthquake engineering. Several key parameters specified in the catalog include magnitude, source-to-site distance, focal depth, and focal mechanism as well as the instrument type. High and low frequencies (FH & FL) were determined for each record (Table 4). The records studied in this paper were

presented based on their code (assigned by the BHRC), station name, site class, corner frequencies, band-pass filter calculated for each record, maximum values of strong ground motion (PGA, PGV, PGD) for three components, event date, coordinates for earthquake and station epicenter, reported magnitude, focal depth, focal mechanism and the hypocentral distances (Table 5). The velocity and displacement time-histories of the records were obtained based on the single and double integration of accelerograms. In addition, the average shear wave velocity in the upper 30 meters, as one of the trusted parameters in classification of soil types, was specified in this article. Classification for local site conditions at each recording site into one of four categories, defined as I, II, III, and IV, were done, and finally 217 triaxial near source strong-motion adequately recorded corresponding to 30 shallow crustal earthquakes were reported for future studies and preparing the response and design spectrum.

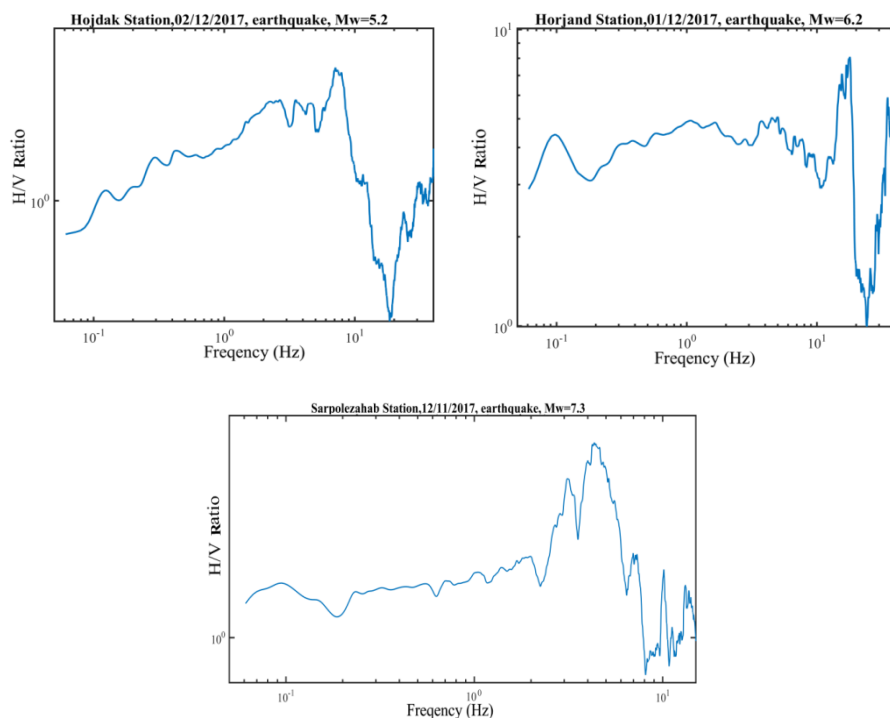


Fig 12. The H/V ratio for Hojedk station, Mw=5.2, 02/12/2017, Horand jstation with Mw=6.2, 01/12/2017, and Sarpolezahab station recorded in 12/11/2017, Mw=7.3 earthquake.

#### 5. Conclusion

Near fault earthquakes have special characteristics. These characteristics make difference between near-fault earthquakes and far-fault earthquakes. Each country susceptible to disasters should have appropriate construction standards and must update its existing building codes. In this regard, special attention must be given to the devastating recent earthquakes and a study of records for analysis of physical properties and

parameters of the earth can thereby reduce vulnerability to natural disasters. Soil has two important characters, one is filtering some of the periods, and the second one is resonance of the earthquakes waves coming from bedrock. The contribution of the present study is gathering the highly qualified strong ground motion near fault records taken in Iran, California and Italy (1976-2018), in different seismotectonic zones and 4 soil types, including earthquake source parameters,

source to site distance, depth, VS30, style of faulting and band pass filtering range. Most of these accelerograms have been recorded in destructive earthquakes in Iran. This data is very important and reflects the interior physical properties of the earth. Therefore, investigating and analyzing them is highly recommended in the seismic design of structures, residential settlements, vital arteries, etc. in each region.

## References

- Aki K (1968) Seismic displacements near a fault, *Journal of Geophysical Research* 73:5359-5376.
- Akbar S, Bommer JJ (2007) Prediction of elastic displacement response spectra in Europe and the Middle East, *Earthquake Engineering & Structural Dynamics* 36:1275-1301.
- Ambraseys N, Melville C (1982) A History of Persian Earthquakes, Cambridge University Press, London.
- Ambraseys N, Smit P, Douglas J, Margaris B, Sigbjörnsson R, Olafsson S, Suhadolc P, Costa G (2004) Internet site for European strong-motion data, *Bollettino di geofisica teorica ed applicata* 45:113-129.
- Boore DM, Zoback MD (1974) Near-field motions from kinematic models of propagating faults, *Bulletin of the Seismological Society of America* 64:321-342.
- Bouchon M (1979) Predictability of ground displacement and velocity near an earthquake fault: An example: The Parkfield earthquake of 1966, *Journal of Geophysical Research: Solid Earth* 84:6149-6156.
- Campbell KW, Bozorgnia Y (2013) NGA-West2 Campbell-Bozorgnia ground motion model for the horizontal components of PGA, PGV, and 5%-damped elastic pseudo-acceleration response spectra for periods ranging from 0.01 to 10 sec. Pacific Earthquake Engineering Research Center,
- Chu D, Gordon RG (1998) Current plate motions across the Red Sea, *Geophysical Journal International* 135:313-328.
- Code IS (2005) Iranian code of practice for seismic resistant design of buildings, *Standard*.
- Council BSS (2000) The 2000 NEHRP recommended provisions for new buildings and other structures: Part I (Provisions) and Part II (Commentary), *FEMA* 368:369.
- Engdahl ER, van der Hilst R, Buland R (1998) Global teleseismic earthquake relocation with improved travel times and procedures for depth determination, *Bulletin of the Seismological Society of America* 88:722-743.
- Forootan M, Silakhoori E, Alvandi E (2015) Soil Liquefaction Hazard Zonation Map for Kordkuy County, Golsetan Province Using Model SWM, *IRANIAN JOURNAL OF EARTH SCIENCES* 7:46-49.
- Gutenberg B, Richter CF (1944) Frequency of earthquakes in California, *Bulletin of the Seismological Society of America* 34:185-188.
- Hanks TC, Kanamori H (1979) A moment magnitude scale, *Journal of Geophysical Research: Solid Earth* 84:2348-2350.
- Hartzell SH (1978) Earthquake aftershocks as Green's functions, *Geophysical Research Letters* 5:1-4.
- Haskell NA (1969) Elastic displacements in the near-field of a propagating fault, *Bulletin of the Seismological Society of America* 59:865-908.
- Israel M, Kovach RL (1977) Near-field motions from a propagating strike-slip fault in an elastic half-space, *Bulletin of the Seismological Society of America* 67:977-994.
- Kramer S (1996) Geotechnical Earthquake Engineering. Prentice-Hall, Inc, *New Jersey*:348-422.
- Levy N, Mal A (1976) Calculation of ground motion in a three-dimensional model of the 1966 Parkfield earthquake, *Bulletin of the Seismological Society of America* 66:405-423.
- Maggi A, Priestley K, Jackson J (2002) Focal depths of moderate and large size earthquakes in Iran, *Journal of Seismology and Earthquake Engineering* 4:1-10.
- Pecknold DA, Riddell R (1978) Effect of initial base motion on response spectra, *Journal of the Engineering Mechanics Division* 104:485-491.
- Theodulidis N, Bard P-Y (1995) Horizontal to vertical spectral ratio and geological conditions: an analysis of strong motion data from Greece and Taiwan (SMART-1), *Soil dynamics and earthquake engineering* 14:177-197.
- Zaré M (2007) Spectral Demand Curves Based on the Selected Strong Motion Records in Iran, *Journal of Seismology and Earthquake Engineering* 9:111-123.